PHYSICAL REVIEW B VOLUME 3, NUMBER 4 15 FEBRUARY 1971

Behavior of the Electronic Dielectric Constant in Covalent and Ionic Materials

S. H. Wemple and M. DiDomenico, Jr.
Bell Telephone Laboratories Incorporated, Murray Hill, New Jersey 07974

(Received 30 July 1970)

Refractive-index dispersion data below the interband absorption edge in more than 100 widely different solids and liquids are analyzed using a single-effective-oscillator fit of the form $n^2-1=E_dE_0/(E_0^2-\hbar^2\omega^2)$, where $\hbar\omega$ is the photon energy, E_0 is the single oscillator energy, and E_d is the dispersion energy. The parameter E_d, which is a measure of the strength of interband optical transitions, is found to obey the simple empirical relationship $E_d=\beta N_c Z_a N_e$, where N_c is the coordination number of the cation nearest neighbor to the anion, Z_a is the formal chemical valency of the anion, N_e is the effective number of valence electrons per anion (usually $N_e=8$), and β is essentially two-valued, taking on the "ionic" value $\beta_i=0.26\pm0.04$ eV for halides and most oxides, and the "covalent" value $\beta_c=0.37\pm0.05$ eV for the tetrahedrally bonded A^NB^{8-N} zinc-blende- and diamond-type structures, as well as for scheelite-structure oxides and some iodates and carbonates. Wurtzite-structure crystals form a transitional group between ionic and covalent crystal classes. Experimentally, it is also found that E_d does not depend significantly on either the bandgap or the volume density of valence electrons. The experimental results are related to the fundamental ϵ_2 spectrum via appropriately defined moment integrals. It is found, using relationships between moment integrals, that for a particularly simple choice of a model ϵ_2 spectrum, viz., constant optical-frequency conductivity with high- and low-frequency cutoffs, the bandgap parameter E_a in the high-frequency sum rule introduced by Hopfield provides the connection between the single-oscillator parameters (E_0, E_d) and the Phillips static-dielectric-constant parameters (E_g, $\hbar\omega_p$), i.e., $(\hbar\omega_p)^2=E_aE_d$ and $E_g^2=E_aE_0$. Finally, it is suggested that the observed dependence of E_d on coordination number and valency implies that an understanding of refractive-index behavior may lie in a localized molecular theory of optical transitions.

I. INTRODUCTION

The fundamental electronic excitation spectrum of a substance is generally described in terms of a frequency-dependent complex electronic dielectric constant $\epsilon(\omega)=\epsilon_1(\omega)+i\epsilon_2(\omega)$. Either the real part ($\epsilon_1$) or the imaginary part (ϵ_2) contains all the desired response information, since causality arguments relate the real and imaginary parts via the well-known Kramers-Kronig (K-K) relations, i.e.,

$$\epsilon_1(\omega)-1=\frac{2}{\pi}\,\mathcal{P}\int_0^\infty \frac{\omega'\epsilon_2(\omega')}{\omega'^2-\omega^2}\,d\omega',$$
$$\epsilon_2(\omega)=-\frac{2\omega}{\pi}\,\mathcal{P}\int_0^\infty \frac{\epsilon_1(\omega')-1}{\omega'^2-\omega^2}\,d\omega', \tag{1}$$

where $\mathcal{P}$ denotes the principal part. In materials exhibiting a bandgap, the real part in the region of transparency below the gap is related to optical absorption above the gap by

$$\epsilon_1(\omega)-1=n^2(\omega)-1=\frac{2}{\pi}\,\mathcal{P}\int_{\omega_t}^\infty \frac{\omega'\epsilon_2(\omega')}{\omega'^2-\omega^2}\,d\omega', \quad \omega<\omega_t \tag{2}$$

where ω_t is the threshold frequency, and we have identified ϵ_1 with the square of the refractive index n. The frequency ω is assumed to lie above all lattice vibrational modes, i.e., only electronic excitations are being considered. In the language of Eq. (2), a theory of the refractive index would entail computation of $\epsilon_2(\omega)$ followed by integration over all frequencies. Although a formal perturbation theory procedure for computing $\epsilon_2(\omega)$ exists within the framework of the one-electron band theory of solids, such computations require integration over the full Brillouin zone as well as over all frequencies, so that important physical quantities tend to be obscured by the computational details of the anaylsis. Furthermore, several adjustable parameters are generally introduced into energy-band calculations, and in the more ionic materials excitonic effects are difficult to account for quantitatively. It is useful, therefore, to approximate the general theoretical expressions for $\epsilon_1(\omega)$ in ways that display explicitly certain physically meaningful parameters. These parameters depend on the particular approximation being made. Phillips[1] and Van Vechten,[1] for example, make use of the Penn model[2] description of the *static* electronic dielectric constant to define an "average energy gap" E_g, whereas we use[3] a single-oscillator description of the *frequency-dependent* dielectric constant to define a "dispersion-energy" parameter E_d. These parameters are useful because they turn out to obey remarkably simple empirical rules in large groups of materials. Although these rules are quite different in detail, one common feature is the overwhelming evidence that both crystal structure and ionicity influence the refractive-index behavior of solids in ways that can be simply described. This

experimental observation should be contrasted with existing theories for which any simple connection between the final result (i.e., the dielectric constant) and crystal structure or ionicity tends to be obscured by the analysis.

In the present article, our purpose is to expand the analysis of refractive-index behavior reported previously.[3] We show how the single-oscillator description is a "natural" approximation to the dielectric response function and compare in detail the single-oscillator and Penn-model parametrization with emphasis on the relationships between moments of the $\epsilon_2(\omega)$ spectrum and the model parameters. Tables of experimental oscillator parameters are presented for nonmetallic ionic and covalent semiconductors and insulators, magnetic insulators, and liquids. These tables enable us to extend the empirical rule reported previously,[3] connecting the dispersion energy E_d with coordination number, valency, and ionicity, to a wider range of materials.

Finally, we discuss the implications of the experimental results on our understanding of electronic structure and chemical bonding in solids and liquids. Within the framework of the constant conductivity model,[3] it is shown that the dispersion energy E_d is simply related to $\epsilon_1(\omega)$ at high frequencies above the $\epsilon_2(\omega)$ cutoff via the f sum rule and the Hopfield sum rule.[4] As a result, E_d is related to the charge distribution within each unit cell and is, thus, a quantity closely related to chemical bonding. The observed simple dependence on coordination number and chemical valency suggests further that nearest-neighbor atomiclike quantities strongly influence the electronic optical properties of materials, and that an understanding of these properties as well as bonding may lie within a nearly localized molecular theory.

II. SINGLE-OSCILLATOR DESCRIPTION OF ELECTRONIC DIELECTRIC CONSTANT

Using time-dependent perturbation theory, the following formal expression for the frequency (ω) dependence of the real part of the electronic dielectric constant can be derived:

$$\epsilon_1(\omega) = 1 + \frac{e^2}{\pi^2 m} \sum_{i,j}{}' \int_{\mathrm{BZ}} d^3k \frac{f_{ij}^{\alpha}(\vec{k})}{\omega_{ij}^2(\vec{k}) - \omega^2} . \qquad (3)$$

Here e and m are, respectively, the electronic charge and mass. The sum extends over all bands i and j such that $i \neq j$, and the integral extends over the volume of the Brillouin zone (BZ). The interband oscillator strength for polarization direction α is given by $f_{ij}^{\alpha}(\vec{k})$. We shall consider two approximations to Eq. (3) which contain parameters that can be measured experimentally. The first is the zero frequency or static-electronic dielectric constant, and the second is the frequency dependence of the dielectric constant in the region of transparency, i.e., $\omega < \omega_{ij}$.

Penn[2] has shown that the static dielectric constant of a semiconductor can be computed using an isotropic free-electron model containing a single energy gap E_g. Apart from a factor of order unity, we can obtain his result from Eq. (3) by letting $\hbar\omega_{ij} \approx E_g$, where E_g is an average energy gap. Equation (3) then becomes

$$\epsilon_1(0) = 1 + \frac{e^2\hbar^2}{\pi^2 m E_g^2} \sum_{i,j}{}' \int_{\mathrm{BZ}} d^3k\, f_{ij}^{\alpha}(\vec{k}) \quad . \qquad (4)$$

Making use of the f sum rule and noting that

$$\sum_j \int_{\mathrm{BZ}} d^3k = 4\pi^3 n_v , \qquad (5)$$

where n_v is the effective density of valence electrons, Eq. (4) reduces to

$$\epsilon_1(0) = 1 + (\hbar\omega_p)^2/E_g^2 . \qquad (6)$$

Here $\omega_p^2 = 4\pi n_v e^2/m$ is the plasma frequency of the valence electrons. Phillips[1] and Van Vechten[1] have shown that the average energy gap E_g can be sensibly decomposed into homopolar and heteropolar parts E_h and C obeying the quadrature relation $E_g^2 = E_h^2 + C^2$ and that new and useful scales of ionicity and electronegativity can be defined within the framework of the single-gap dielectric model. Furthermore, these authors have also shown that a remarkably wide range of experimental observations in many materials can be correlated using a "small number" of adjustable parameters associated with E_g.[5]

To calculate the frequency dependence of the dielectric constant we note that for a single group of valence and conduction bands Eq. (3) can be rewritten as

$$\epsilon_1(\omega) = 1 + \frac{4\pi e^2}{m\Omega} \sum_{\vec{k}} \frac{f_{cv}^{\alpha}(\vec{k})}{\omega_{cv}^2(\vec{k}) - \omega^2} , \qquad (7)$$

where Ω is the volume of the crystal, and c and v denote conduction and valence bands. If we approximate the important interband transitions in the BZ by individual oscillators and recognize that each valence electron contributes one such oscillator, Eq. (7) may be approximated by

$$\epsilon_1(\omega) = 1 + \omega_p^2 \sum_n \frac{f_n}{(\omega_n^2 - \omega^2)} . \qquad (8)$$

Equation (8) has the same form as the classical Kramers-Heisenberg dispersion formula for an assembly of weakly interacting atoms. In Eq. (8), f_n is the electric-dipole oscillator strength associated with transitions at frequency ω_n. The summation over oscillators ω_n can be sensibly approximated for $\omega < \omega_n$ by isolating the first (strong) oscillator $f_1/(\omega_1^2 - \omega^2)$ and combining the remaining terms

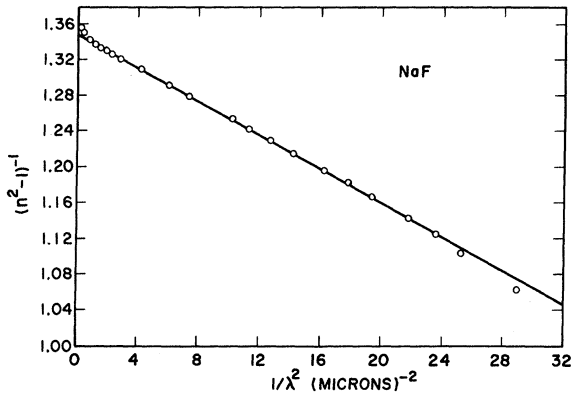

FIG. 1. Plot of refrective-index factor $(n^2-1)^{-1}$ versus λ^{-2} for NaF.

in the form

$$\sum_{n\neq 1} (f_n/\omega_n^2)\,(1+\omega^2/\omega_n^2).$$

Combining these higher-order contributions with the first-resonant oscillator and retaining terms to order ω^2 then yields the single-oscillator approximation

$$\epsilon_1(\omega)-1 \approx F/[E_0^2-(\hbar\omega)^2]\,, \tag{9}$$

where the two parameters E_0 and F are related straightforwardly to all the f_n and ω_n in Eq. (8). Equation (9) provides a two-parameter approximation at low energies $\omega \lesssim \omega_t$ to the theoretical result expressed by Eq. (3). The usefulness of Eq. (9) depends, of course, on affirmative answers to the following two questions: (i) Do real solids obey the single-oscillator approximation with "reasonable" accuracy; and (ii) do the experimentally observed values of the parameters E_0 and F (or some combination) provide new insights into the optical properties of matter? In an earlier paper,[3] we asserted that a positive answer could be given to the first question for more than 50 widely different ionic and covalent nonmetallic crystals, and we showed experimentally that a special combination of parameters ($E_d = F/E_0$) obeyed an extraordinarily simple empirical relation for this same large group of materials. In terms of the dispersion energy E_d, Eq. (9) can be rewritten in the form

$$n^2(\omega)-1 = E_d E_0/[E_0^2-(\hbar\omega)^2]\,. \tag{10}$$

Experimental verification of Eq. (10) can be obtained by plotting $1/(n^2-1)$ versus ω^2 (or λ^{-2}). The resulting straight line then yields values of the parameters E_0 and E_d . Some typical results are shown in Figs. 1-3 for NaF, $Ba_2NaNb_5O_{15}$, and CdS. These curves illustrate the general features observed in a total of over 100 materials investigated to date. At long wavelengths, a positive curvature deviation from linearity is usually observed due to the negative contribution of lattice vibrations to the refractive index. At short wavelengths, a negative curvature deviation is sometimes observed due to the proximity of the band edge or excitonic absorption. The largest deviations occur when strong exciton peaks are present below the interband edge, as in CdS (see Fig. 3). However, in all materials studied (both solids and liquids), a sufficiently extended region of linearity is observed to allow unambiguous experimental determination of the two parameters E_0 and E_d. In the worst case (CdS), linearity extends over a factor of 4 in ω^2, and the quantity $(n^2-1)^{-1}$ is depressed approximately 15% below the linear extrapolation close to the absorption (exciton) threshold.

In addition to the single-oscillator parametrization given by Eq. (10), many other curve-fitting forms involving three or more parameters have been used in the literature to describe refractive-index dispersion data. In general, no physical significance has been attached to the parameters, and the expressions serve primarily as interpolation formulas. Our justification for using Eq. (10), apart from its experimental validity, is the *a posteriori* argument that the parameters obtained have fundamental physical significance.

III. RELATIONSHIP OF PARAMETERS TO FUNDAMENTAL $\epsilon_2(\omega)$ SPECTRUM

A simple connection between the single-oscillator parameters E_0 and E_d and the $\epsilon_2(\omega)$ spectrum can be obtained by equating Eq. (10) with Eq. (1) and comparing terms in an expansion in powers of ω^2. The resulting relationships can be compactly expressed in terms of moments of the $\epsilon_2(\omega)$ spectrum. We define the rth moment of the optical spectrum by the relation[3]

$$M_r = (2/\pi)\int_{E_t}^{\infty} E^r \epsilon_2(E)\,dE, \tag{11}$$

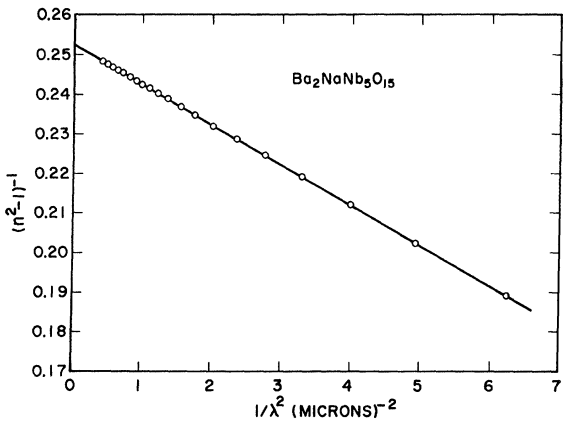

FIG. 2. Plot of refractive-index factor $(n^2-1)^{-1}$ versus λ^{-2} for $Ba_2NaNb_5O_{15}$.

where $E \equiv \hbar\omega$, and E_t is the absorption threshold energy. It should be noted that the definition of moments given here differs somewhat from the definition used in Ref. 3. The parameters E_0 and E_d are then given by

$$E_0^2 = M_{-1}/M_{-3} \tag{12}$$

and

$$E_d^2 = M_{-1}^3/M_{-3} . \tag{13}$$

The oscillator energy E_0 is independent of the scale of ϵ_2 and is consequently an "average" energy gap, whereas E_d depends on the scale of ϵ_2, and thus serves as an interband strength parameter. Since the -1 and -3 moments are involved in computation of E_0 and E_d, the ϵ_2 spectrum is weighted most heavily near the interband absorption threshold. It is instructive to compare Eqs. (12) and (13) with corresponding expressions for the quantities $\hbar\omega_p$ and E_g entering into the Phillips-dielectric model. Using the f-sum-rule integral and the K-K relation, it is easy to show that

$$(\hbar\omega_p)^2 = M_1 , \tag{14}$$

and

$$E_g^2 = M_1/M_{-1} . \tag{15}$$

The Phillips "bandgap" E_g is, thus, simply the ratio of the +1 to the −1 moments, and consequently weights the ϵ_2 spectrum at higher energies more heavily than the corresponding expression for E_0 given by Eq. (12). Interband transition strengths are described by the plasma energy M_1 in this model, whereas the single-oscillator model uses the quantity M_{-1}^3/M_{-3} to describe transition strengths.

Hopfield[4] has recently derived a new sum rule relating optical properties to the charge distribution within a unit cell. He introduces the energy-gap parameter E_a defined by the moment relation

$$E_a^2 = M_3/M_1 , \tag{16}$$

and shows that this energy is related to an integral of the product of the Laplacian of the bare crystal potential and the fluctuation in the electron density. The symmetry in the expressions for E_0, E_g, and E_a is evident in Eqs. (12), (15), and (16), as is the inequality

$$E_t < E_0 < E_g < E_a . \tag{17}$$

Other "average" energy gaps can be defined by the general relation $E_r^2 = M_r/M_{r-2}$, although thus far only the gaps E_0, E_g, and E_a have been found useful.

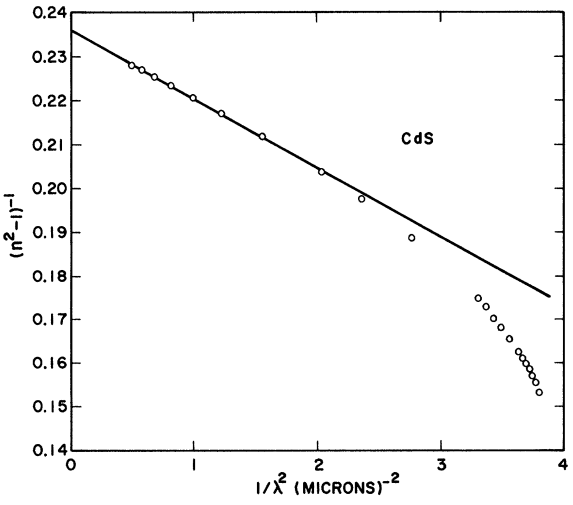

FIG. 3. Plot of refractive-index factor $(n^2-1)^{-1}$ versus λ^{-2} for CdS.

IV. OTHER PARAMETRIZATIONS OF REFRACTIVE INDEX

A third parametrization of refractive-index behavior that has gained wide acceptance is the Clausius-Mossotti local-field polarizability model.[6] This description introduces physically appealing quantities (i.e., the Lorentz local-field factor Γ and the electronic polarizability α), but these quantities are not separately measureable, in general, nor can they be computed from fundamental theories. In terms of α and Γ, the zero-frequency refractive index can be expressed in the form

$$n^2(0) - 1 = 4\pi N \sum_i \alpha_i \Big/ (1 - N \sum_i \Gamma_i \alpha_i), \tag{18}$$

where α_i and Γ_i are the electronic polarizabilities and local-field factors for the ith atom in each unit cell, and N is the volume density of unit cells. For a cubic array of isolated ions, $\Gamma = \frac{4}{3}\pi$, and Eq. (18) reduces to the well-known Lorentz-Lorenz form

$$(n^2 - 1)/(n^2 + 2) = \tfrac{4}{3}\pi N \alpha_0 , \tag{19}$$

where $\alpha_0 = \sum_i \alpha_i$. In most solids neither the assumption of cubic symmetry nor isolated ions is valid. In the covalent limit, extreme overlap between nearest-neighbor wave functions gives $\Gamma \to 0$.[7] The Lorentz factor is, thus, clearly related in some way to ionicity as well as structure. There is, however, no fundamental theory that allows quantitative determination of Γ in solids that are not strongly ionic. For this reason a value for Γ is often assumed, and the total polaribility α_0 is then determined experimentally from Eq. (18). Such a procedure is useful provided polarizabilities are additive and provided they have essentially the same value for each ion when placed in a variety of crystalline and chemical environments. This turns out to be limited to certain families of ionic crystals,[6] so that Eq. (18), apart perhaps from giving useful qualitative insights, does not yield parameters that can always be unambiguously measured nor are the parameters necessarily applicable to large groups of crystals. It is of interest to note in passing that a sin-

gle-oscillator description of α_0 in the Lorentz-Lorenz expression [see Eq. (19)] cannot be distinguished experimentally from a single-oscillator description of n^2-1.

Another parametrization of refractive-index data that is sometimes used involves normalization of various functions of the refractive index [e.g., $n-1$ or $(n^2-1)/(n^2+2)$] by the density. Although a variety of empricial rules are observed to apply to groups of complex materials, it is difficult to ascribe physical significance to the resulting parameters. The reader is referred to the book by Batsonov[8] for a detailed presentation of this "refractometry" approach.

V. EXPERIMENTAL RESULTS

Using available refractive-index-dispersion data, we have computed the single-oscillator parameters E_0 and E_d for over 100 solids and liquids. The results, listed in Tables I–IV are grouped into the following four categories: Table I, nonmagnetic crystals containing a single anion species; Table II, nonmagnetic crystals containing anion radicals; Table III, magnetic crystals; and Table IV, liquids. For brevity we have included values of E_0 and E_d for only one direction of light polarization in uniaxial and biaxial crystals. In most cases, E_d is found to be very nearly isotropic.

A. Table I – Nonmagnetic Crystals Containing a Single Anion Species

The crystals in Table I are grouped into separate subgroups according to the formal anion valency (Z_a), the coordination number of the *nearest-neighbor* cation (N_c), and the effective number of valence electrons per anion (N_e). We take $N_e \equiv 8$ in all compounds containing only filled s-p valence bands. This would include, in the tetrahedrally coordinated $A^N B^{8-N}$ covalent compounds, all 8 electrons in the directed sp^3 hybridized orbitals. An argument for taking $N_e \equiv 6$ in ionic crystals is given in Sec. VII, although we have not done so in the tabulations. As discussed below and in Ref. 3, some complicating features occur in the thalium halides ($N_e = 10$) and in the noble metal salts ($N_e \approx 18$).

We now turn to the values of E_d listed in Table I and make the following pertinent observations.

(a) The parameter E_d in ten six-coordinated alkali halides (excluding LiF) has very nearly the same value of 12.6 ± 1.4 eV, although the oscillator energy E_0 varies by a factor of 2 and the unit cell volume varies by a factor of 4. The value of E_d for LiF appears to fall slightly outside the listed limits.

(b) In the eight-coordinated CsCl- and CaF_2-type structures, $E_d = 16.2 \pm 1$ eV. This value is very nearly a factor $\frac{8}{6}$ times that observed in the six-coordinated structures. A simple proportionality between E_d and N_c is thus implied by this result. Note in particular the values of E_d for six- and eight-coordinated CsCl.

(c) The parameter E_d in 15 six-coordinated oxides in which E_0 varies by a factor of 2.5 is 24.7 ± 2.8 eV. This factor-of-two difference between six-coordinated oxides and halides suggests the possibility of a simple proportionality between E_d and Z_a.

(d) The parameter E_d in five four-coordinated oxides (17.7 ± 0.6 eV) is about $\frac{4}{6}$ times its value in the six-coordinated oxides, thus lending further support to the view that E_d is approximately proportional to N_c.

(e) The four scheelite-structure oxides ($N_c = 4$) listed in Table I have $E_d = 22.3 \pm 1.0$ eV. This value is considerably larger than that noted above for other four-coordinated oxides ($E_d = 17.7 \pm 0.6$ eV). As a result, the scheelite crystals do not appear to fall within the simple framework of a proportionality between E_d and N_c. It should be noted that other nonscheelite crystals containing MoO_4 tetrahedra have values of E_d in line with a proportionality between E_d and N_c [e.g., $E_d \approx 18.4$ eV in $Gd_2(MoO_4)_3$ and $Tb_2(MoO_4)_3$]. There are at least two explanations for the unusual behavior of scheelites. First, it is possible that the divalent cations (Ca, Pb, Sr), which are essentially eight-coordinated, contribute somewhat to optical transitions and raise E_d above its four-coordinated value. Second, the tetrahedra in the scheelite structure may be more covalently bonded than in nonscheelites. We will return to this point below.

(f) The parameter E_d has the value 26 ± 1 eV in four II–IV compounds ($Z_a = 2$) having the zinc-blende structure. In the three III–V compounds ($Z_a = 3$), E_d is approximately a factor $\frac{3}{2}$ larger, and in the IV–IV compounds ($Z_a = 4$), E_d is approximately a factor of 2 larger. There thus appears to be at least an approximate proportionality between E_d and Z_a even in the covalent tetrahedrally coordinated binary compounds. We have excluded small-band-gap and impure materials from this listing because free carrier and donor (or acceptor) photo-ionization absorption can contribute significantly to the apparent dispersion of the refractive index, and thus to E_d. Such effects may in fact influence the listed value of E_d for Ge.

(g) The parameter E_d is about 21 eV in the eight-coordinated thalium halides. This value is approximately a factor $\frac{10}{8}$ times that observed in the isostructural alkali halides. We attribute this difference to the extra $6s^2$ electrons associated with the Tl^+ ion. Thus, for the thalium salts we take $N_e \equiv 10$ and assume that E_d is proportional to N_e.

(h) The noble-metal salt AgCl crystallizes in the NaCl-type structure, yet the observed value of E_d is larger by nearly a factor of 2, i.e., E_d has the value expected for a six-coordinated oxide. Similarly, E_d in four-coordinated CuCl is the same as

TABLE I. Dispersion parameters for nonmagnetic crystals containing a single anion species.

Crystal	E_0(eV)	E_d(eV)	β(eV)
NaCl type ($N_c=6$, $Z_a=1$, $N_e=8$)			
LiF	17.1	14.9	0.31
NaF	15	11.3	0.24
KF	14.8	12.3	0.26
NaCl	10.3	13.6	0.28
KCl	10.5	12.3	0.26
RbCl	10.4	12.2	0.25
CsCl	10.6	14.0	0.29
KBr	9.2	12.4	0.26
RbBr	9.1	12.1	0.25
KI	7.7	12.8	0.27
RbI	7.7	12.1	0.25
CsCl type ($N_c=8$, $Z_a=1$, $N_e=8$)			
CsCl	10.6	17.1	0.27
CsBr	9.4	17.0	0.27
CsI	7.5	15.2	0.24
CsCl type ($N_c=8$, $Z_a=1$, $N_e=10$)			
TlCl	5.8	20.6	0.26
TlBr	5.3	21.7	0.27
CaF_2 type ($N_c=8$, $Z_a=1$, $N_e=8$)			
CaF_2	15.7	15.9	0.25
BaF_2	13.8	15.9	0.25
Noble-metal salts ($Z_a=1$, $N_e=18$)			
AgCl ($N_c=6$)	7.4	22	0.20
CuCl ($N_c=4$)	8.3	18.6	0.26
Wurtzites ($N_c=4$, $Z_a=2$, $N_e=8$)			
ZnO	6.4	17.1	0.27
CdS	4.9	20.4	0.32
CdSe	4.0	20.6	0.32
ZnS	6.15	25.2	0.39
Oxides ($N_c=6$, $Z_a=2$, $N_e=8$)			
MgO	11.3	22	0.23
CaO	9.9	22.6	0.24
Al_2O_3	13.4	27.5	0.29
$Y_3Al_5O_{12}$	11.1	25.4	0.26
TeO_2	6.24	23.2	0.24
$SrTiO_3$	5.68	23.7	0.25
$BaTiO_3$	5.63	24.0	0.25
$KTaO_3$	6.50	23.7	0.25
$KTa_{0.65}Nb_{0.35}O_3$	6.17	23.4	0.25
$LiTaO_3$	7.49	26.1	0.27
$LiNbO_3$	6.65	25.9	0.27
$Ba_2NaNb_5O_{15}$	6.19	24.4	0.26
TiO_2	5.24	25.7	0.27
$MgAl_2O_4$	12.1	23.3	0.27
$ZnWO_4$	7.46	26.0	0.27

TABLE I. (*continued*)

Crystal	E_0(eV)	E_d(eV)	β(eV)
Oxides ($N_c=4$, $Z_a=2$, $N_e=8$)			
ZnO	6.4	17.1	0.27
SiO_2	13.6	18.3	0.29
$LiGaO_2$	9.5	18.1	0.28
$Gd_2(MoO_4)_3$	8.3	18.5	0.29
$Tb_2(MoO_4)_3$	8.1	18.4	0.29
Oxides (scheelite structure) ($N_c=4$, $Z_a=2$, $N_e=8$)			
$CaWO_4$	9.15	23.3	0.36
$CaMoO_4$	8.26	23.0	0.36
$PbMoO_4$	5.4	22.6	0.35
$SrMoO_4$	8.6	21.3	0.33
Zinc blende ($N_c=4$, $Z_a=2$, $N_e=8$)			
ZnS	6.36	26.1	0.41
ZnSe	5.54	27.0	0.42
ZnTe	4.34	27.0	0.42
CdTe	4.13	25.7	0.40
Zinc Blende ($N_c=4$, $Z_a=3$, $N_e=8$)			
GaP	4.46	36.0	0.38
GaAs	3.55	33.5	0.35
$ZnGeP_2$	4.04	35.2	0.37
Diamond type ($N_c=4$, $Z_a=4$, $N_e=8$)			
C	10.9	49.7	0.39
β SiC	7.6	42	0.33
Si	4.0	44.4	0.35
Ge	2.7	41	0.32

observed in four-coordinated oxides (ZnO and SiO_2). We attribute the occurrence of anomalously large values of E_d in these noble-metal salts to contributions of the filled d band to interband transitions, and thus take $N_e \approx 18$.

(i) The parameter E_d in four II–VI wurtzite-structure crystals varies between 17.1 (ZnO) and 25.2 eV (ZnS). We will comment on this observation below.

As suggested in Ref. 3, the above observations lead us to conclude that the quantity

$$\beta = E_d/N_c Z_a N_e \text{ eV} \tag{20}$$

has very nearly the same numerical value in large groups of crystals containing a single anion species. In particular, we find from Table I that β is essentially two-valued, taking on the "ionic" value β_i for halides and most oxides (scheelites being an exception as noted above), i.e.,

$$\beta_i = 0.26 \pm 0.04 \text{ eV}, \tag{21}$$

and taking on the "covalent" value β_c in the zinc-

blende, scheelite, and diamond-type structures, i.e.,

$$\beta_c = 0.37 \pm 0.05 \text{ eV}. \quad (22)$$

The wurtzite-structure crystals appear to range between the ionic and covalent extremes with ZnO falling at the ionic limit and ZnS at the covalent limit. Thus, it would appear based solely on experimental values of E_d that large groups of crystals containing a single anion species can be grouped into distinct ionic and covalent classes with wurtzite crystals forming a transitional group between these extremes. This rather remarkable result has also been noted within the ionicity scale of Phillips and Van Vechten. Furthermore, Kurtin *et al.*[9] deduced the existence of distinct ionic and covalent crystal classes based on observations of barrier energies at metal-semiconductor interfaces, exciton strengths, and the relative importance of "direct" and "nondirect" transitions. These authors also find that wurtzite-structure crystals form a transitional group between covalent and ionic crystal classes.

Turning to the oxides, it is of interest that all the six-coordinated oxides have the ionic value of $\beta = \beta_i$, whereas the four-coordinated oxides seem to be either ionic or covalent (scheelites). Although it is possible that the four-coordinated oxides, in analogy with the wurtzites, fall near the ionic-covalent transition with scheelites on the covalent side, this explanation cannot be distinguished from that suggested above attributing the larger E_d value in scheelites to the influence of the divalent cation-oxygen bond.

B. Table II – Nonmagnetic Crystals Containing Anion Radicals

In Table II we list values of E_0, E_d, and β for a representative sample of nonmagnetic crystals containing XO_m anion radicals. If we continue to define β by Eq. (20) and take for N_c the coordination number of the nearest-neighbor X ion (e.g., Cl, C, P, I), the values of β shown in Table II are obtained. Although no general rules can be deduced because of the limited number of crystals listed and the restricted wavelength range of the data, the results shown in Table II are clearly reminiscent of those tabulated in Table I. Thus, the nitrates, phosphates, sulphates, and chlorates appear to have the ionic β value ($\beta_i = 0.26 \pm 0.04$ eV), whereas the iodates and carbonates have the covalent value ($\beta_c = 0.37 \pm 0.05$). It is of interest that the single periodate listed (KIO_4) appears to fall into the ionic class. These experimental results suggest that the simple empirical rule expressed by Eqs. (20)–(22) may apply to many, if not most, crystalline solids containing anion radicals, and that even in these materials coordination number and ionicity are simply related to refractive-index dispersion.

TABLE II. Dispersion parameters for nonmagnetic crystals containing anion radicals.

Crystal	N_c	E_0(eV)	E_d(eV)	β(eV)
KH_2PO_4	4	12.8	16	0.25
$NH_4H_2PO_4$	4	12.2	16	0.25
$AlPO_4$	4	13.9	18	0.28
KNO_3	3	13.5	10.3	0.22
$NaNO_3(\perp)$[a]	3	8.5	12.1	0.25
$NaNO_3(\parallel)$[a]	3	15	11.5	0.24
$Ba(NO_3)_2$	3	9.6	13.4	0.28
K_2SO_4	4	13.8	16.5	0.26
Rb_2SO_4	4	13.8	17.5	0.27
$LiKSO_4$	4	15.8	14.0	0.22
$NaClO_4$	4	12.4	15.4	0.24
$RbClO_4$	4	14.5	16.4	0.26
NH_4ClO_4	4	13.6	15.4	0.24
Rb_2SeO_4	4	12.2	16.7	0.26
KIO_4	4	9.1	14	0.22
HIO_3	3	7.6	21	0.44
$LiIO_3$	3	8.34	20	0.42
$SrCO_3$	3	15.2	19.8	0.41
$CaCO_3$	3	10.9	18.5	0.39

[a] We include for $NaNO_3$ data for light polarized parallel ($\parallel$) and perpendicular ($\perp$) to the uniaxial c axis. Note that E_d is very nearly isotropic despite a large anisotropy in E_0.

C. Table III – Magnetic Crystals

In Table III we show values of E_0 and E_d for the magnetic europium chalcogenides. The value of E_d in EuO (9 eV) is much lower than in isostructural MgO (22 eV). Furthermore, there is a monotonic increase in E_d in going from the oxide to the telluride. These results fall outside the framework of Tables I and II; however, they can be easily understood by taking into account the $4f^7 \rightarrow 4f^6(5d)$ transitions as well as transitions between the s-p valence band and the d-like conduction band. Transitions originating from the $4f$ electrons are responsible for the observed bandgap and contribute substantially to dispersion of the refractive index. The higher-energy transitions originating in the s-p valence band are the major contributors to the long wavelength refractive index. The above statements can be made quantitative by using a two-oscillator description of the refractive-index dispersion, i.e.,

$$n^2 - 1 = \frac{\hat{E}_d \hat{E}_0}{\hat{E}_0^2 - E^2} + \frac{E_d E_0}{E_0^2 - E^2}, \quad (23)$$

where $\hat{E}_d$, $\hat{E}_0$ applies to the $f \rightarrow d$ transitions and E_d, E_0 applies to the $s, p \rightarrow d$ transitions. It is straightforward to combine terms in Eq. (23) and arrive at the following expressions for the equivalent single-oscillator parameters $\overline{E}_0$ and $\overline{E}_d$:

TABLE III. Dispersion parameters for magnetic crystals.

Crystal	E_0(eV)	E_d(eV)
EuO	2.46	9
EuS	4.0	14
EuSe	4.3	18
EuTe	4.3	21

$$\bar{E}_0^2 = \hat{E}_0^2\left(\frac{1+(E_d/\hat{E}_d)(\hat{E}_0/E_0)}{1+(E_d/\hat{E}_d)(\hat{E}_0/E_0)^3}\right) \tag{24}$$

and

$$\bar{E}_d^2 = \hat{E}_d^2\left(\frac{[1+(E_d/\hat{E}_d)(\hat{E}_0/E_0)]^3}{1+(E_d/\hat{E}_d)(\hat{E}_0/E_0)^3}\right) . \tag{25}$$

To give a numerical example, we take the EuO values for $\bar{E}_0$ and $\bar{E}_d$ listed in Table III, assume that $\hat{E}_0 \approx 1.9$ eV from the photoemission experiments of Eastman *et al.*,[10] and assume further that $E_d \approx 25$ eV based on the E_d values observed in the nonmagnetic six-coordinated oxides. We then find, using Eqs. (24) and (25), that $\hat{E}_d \approx 1.5$ eV, and $E_0 \approx 10$ eV. Similar calculations for EuS yield $\hat{E}_d \approx 2$ eV and $E_0 \approx 8$ eV, and for EuSe, $\hat{E}_d \approx 2$ eV and $E_0 \approx 7$ eV. The calculated values of E_0 are similar to those observed in nonmagnetic six-coordinated crystals (see Table I). Thus, the refractive-index behavior of these magnetic materials containing f electrons can be understood as arising from strong interband ($p \rightarrow d$) transitions at high energy ($E_d \approx 25$ eV) and much weaker $f \rightarrow d$ transitions ($\hat{E}_d \approx 2$ eV) occurring near the absorption threshold at lower photon energies.

D. Table IV – Liquids

We show in Table IV experimental values of E_0 and E_d for several liquids. All of the listed E_d values except for CH_2I_2 fall in the range $E_d = 10 \pm 2$ eV. The relatively low refractive indices observed in these liquids, when compared with many solids, are thus a consequence of weak optical transition strengths as measured by the dispersion energy E_d. A connection between E_d and the coordination number is, of course, complicated in liquids by uncertainties as to the short-range order. If we make the reasonable assumption that molecules remain intact in the liquid so that nearest-neighbor coordination is a valid concept, we then find for CCl_4 (taking $N_e = 8$, $Z_a = 1$, $N_c = 4$) that $\beta = 0.38$ eV, and we find for CS_2 (taking $N_e = 8$, $Z_a = 2$, $N_c = 2$) that $\beta = 0.34$ eV. Both liquids thus display the β value found in covalent solids. A complication occurs for water where the proton lies between two oxygen atoms at a distance 1 Å from the nearest neighbor and 1.7 Å from the next-nearest neighbor.[11] For this situation, the appropriate coordination number is not clearly defined but certainly falls between 1 and 2. By taking $N_e = 8$, $Z_a = 2$ we find $\beta = 0.31$ eV for $N_c = 2$ and $\beta = 0.62$ eV for $N_c = 1$, thus bracketing the crystalline covalent value of $\beta_c = 0.37 \pm 0.05$ eV. For the organic liquids included in Table IV, it is not clear that N_c and Z_a can be sensibly defined so as to provide a useful ordering of the data. In summary, the refractive-index behavior of some inorganic liquids appears to fit well into the framework observed for inorganic solids, although more refractive-index data are clearly required to draw firm conclusions.

VI. EMPIRICAL RULES

The refractive-index dispersion behavior of more than 100 solids and liquids, summarized in Tables I–IV, falls into a remarkably simple pattern. Apart from some liquids for which nearest-neighbor coordination number may be a poorly defined concept, the dispersion energy E_d obeys the empirical relations given by Eqs. (20)–(22). Wurtzite-structure crystals are found to form a transitional group between distinct ionic and covalent crystal classes (four-coordinated oxides may also form a transitional group). Equation (20) expresses the striking result that the influence of structure, chemistry, and ionicity on E_d is simply related to the associated discreet quantities N_c, Z_a, and β. We emphasize that the dependence on anion valency is not limited to ionic materials, but holds also for the tetrahedrally coordinated $A^N B^{8-N}$ covalent compounds. We emphasize also that Eq. (20) contains the following very important implicit observations: (i) E_d is independent of the absorption threshold E_t (bandgap) to within the indicated error limits of ±15%; and (ii) E_d is independent of the lattice constant (or density) to within these same error limits. The first observation imposes constraints on the form of the $\epsilon_2(\omega)$ spectra as discussed in Sec. VII. The second observation places the dispersion energy E_d in a separate category from all other known parametrizations of refractive-index behavior. For example, the volume density of valence electrons is central to the Phillips description (via the plasma energy), the Claussius-Mossotti model, and all refractometry approaches. Because the volume

TABLE IV. Dispersion parameters for liquids.

Liquid	E_0(eV)	E_d(eV)
H_2O	13.0	9.9
CCl_4	11.2	11.2
CS_2	6.9	10.7
C_6H_6 (benzene)	8.9	10.5
C_6H_5OH (phenol)	8.6	11.1
C_2H_5OH (ethyl alcohol)	10.5	10.7
CH_3OH (methyl alcohol)	12.5	9.3
C_5H_{12} (pentane)	10.6	8.3
C_9H_7N (chirolin)	7.4	11.1
CH_2I_2	7.7	14.5

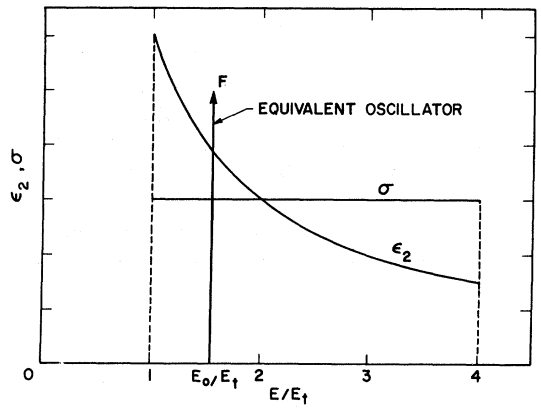

FIG. 4. Model dielectric functions ϵ_2 and σ together with equivalent single oscillator for $b=4$.

density is not required, Eq. (20) provides a useful basis for predicting and understanding the magnitudes of refractive indices in new materials. For example, the long-wavelength value $n(0)$ is given by

$$n^2(0)-1=E_d/E_0=\beta N_c Z_a N_e/E_0 . \tag{26}$$

The oscillator energy E_0 is, to a fair approximation, related empirically to the lowest *direct* bandgap E_t by

$$E_0\approx 1.5\,E_t , \tag{27}$$

so that for ionic compounds

$$n^2(0)-1\approx N_c Z_a N_e/6E_t , \tag{28}$$

and for covalent compounds

$$n^2(0)-1\approx N_c Z_a N_e/4E_t . \tag{29}$$

Equations (28) and (29) provide a more widely applicable connection between bandgaps and refractive indices than that given by Moss's rule[12] and reveal explicitly the importance of coordination number, valency, and ionicity. It is of interest to note that Eqs. (20) and (27), together with Eq. (10), provide a general means for estimating both the magnitude and dispersion of the refractive index in terms of the lowest direct bandgap.

VII. DIELECTRIC MODELS

As noted above, E_d is almost independent of the threshold energy E_t. This result imposes constraints on the ϵ_2 spectrum via the moment integrals contained in Eq. (13). We now consider various model ϵ_2 spectra that satisfy this constraint and compare these spectra with those observed experimentally. Comparison will then be made between the model spectrum derived from dispersion data and the Penn model ϵ_2 spectrum derived theoretically[13] using a simplified single-gap model of the isotropic three-dimensional electron gas.

In Ref. 3 we proposed a simple model spectrum that automatically forces E_d to be independent of E_t, viz., constant-optical-frequency conductivity with high- and low-frequency cutoffs:

$$\begin{aligned} &E\epsilon_2=4\pi\hbar\sigma, \quad E_t<E<bE_t \\ &\epsilon_2=0, \qquad E<E_t \text{ and } E>bE_t . \end{aligned} \tag{30}$$

In Eq. (30), b is an initially arbitrary bandwidth parameter, and σ is the optical conductivity. The model spectrum described by Eq. (30) is shown in Fig. 4 for $b=4$. Also shown is the single oscillator that produces equivalent dispersion of the refractive index for $E\lesssim E_t$.

It has been pointed out recently by Aslaksen[14] that the constant-conductivity model is the simplest member of a general class of ϵ_2 spectra obeying the requirement that E_d be independent of E_t. The form proposed by Aslaksen is

$$\epsilon_2(E)=E_t^{-1}\,g(E/E_t), \tag{31}$$

where $g(E/E_t)$ is an arbitrary function of the normalized photon energy. The constant-conductivity model, for example, requires that $g=4\pi\hbar(E/E_t)^{-1}$. Equation (31) imposes the implicit constraint that the area under the $\epsilon_2(E)$ spectrum for a given class of materials is a constant independent of E_t. Aslaksen has also pointed out that an ϵ_2 spectrum approximated by a series of δ functions, i.e.,

$$\epsilon_2=\sum \alpha_i\delta(E-a_iE_t), \quad a_i\geq 1 \tag{32}$$

satisfies the constraint, in which case

$$E_d^2=\left(\frac{2}{\pi}\right)^2 \left[\sum_i(\alpha_i/a_i)\right]^3/\sum_i(\alpha_i/a_i^3) . \tag{33}$$

For the constant-conductivity model, it has been shown[3] that

$$E_d=8\sqrt{3}\,\hbar\sigma(b-1)/(1+b+b^2)^{1/2} . \tag{34}$$

It is clear that refractive-index dispersion data alone cannot distinguish between these or other dielectric models obeying Eq. (31).

To make a sensible choice we must examine the ϵ_2 spectra of real materials. When this is done we find that many of the available spectra appear to have the following common features: (a) There is a continuous background which increases towards the bandgap and is governed approximately by the expression $\epsilon_2=4\pi\sigma/\omega$; (b) relatively sharp structure is superimposed on this constant-conductivity background; and (c) the spectra cut off rapidly at high frequencies. The structure is related to interband critical points and possibly excitons in ionic materials. Several typical ϵ_2 spectra are shown in Figs. 5–8. Figures 5 and 6 give data for the ionic crystals NaCl[15] and MgO,[16] while Figs. 7 and 8 give data for the covalent crystals Si[17] and GaP.[18] In each figure the approximate constant conductivity background is indicated by a dashed line, and the average oscillator position E_0 is shown by an arrow. The

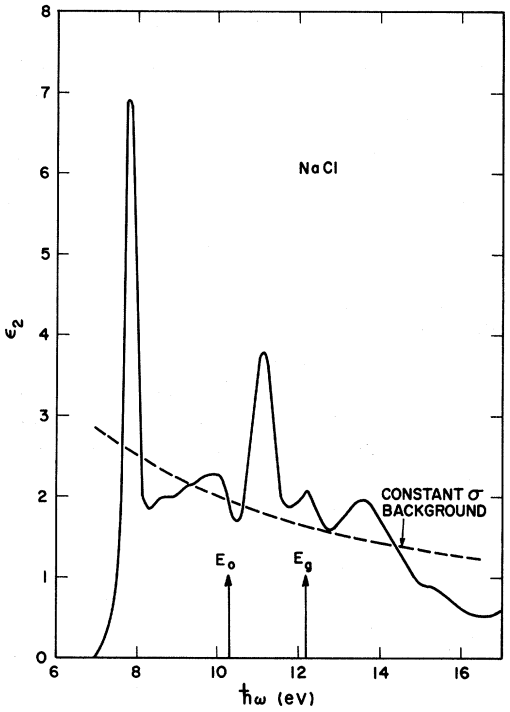

FIG. 5. Experimental ϵ_2 spectrum for NaCl taken from Ref. 15 together with approximate constant-conductivity background and average energy gaps E_0 and E_g.

Phillips bandgap parameter E_g is also indicated. Based on these and other similar, though limited, data we suggest that a reasonable model ϵ_2 spectrum for many materials consists of a superposition of a constant-conductivity background [Eq. (30)] and critical point and/or excitonic structure [Eq. (32)]. This raises the question as to whether the background or the structure determines the value of E_d. Clearly the structure-related quantities (α_i, a_i) are not expected to be the same for all members of a crystal group having the same values of N_c, Z_a, and N_e. For example, among the oxides having $N_c = 6$ the titanates, niobates, and tantalates have d-like conduction bands, whereas s-like bands are found in MgO, CaO, and Al_2O_3. Furthermore, sharp excitons are observed in MgO while excitons are not observed in the niobates and tantalates. Also, the oxygen anion coordination number is 2 in all the listed titanates, niobates, and tantalates, while in MgO and CaO the oxygen coordination number is 6. This same argument applies also to CsCl- and CaF_2-type halides ($N_c = 8$) in which the halide anion coordination numbers are 8 and 4, respectively. Figures 5–8 clearly show that the background is the major contributor to ϵ_2 near the bandgap, and from the moment integrals in Eq. (13), it is this portion of the ϵ_2 spectrum that makes the largest contribution to E_d. We therefore suggest, to within ±15% limits, that the behavior of the refractive index below the interband edge is determined primarily by the approximate constant-conductivity background and that the critical-point (and/or excitonic) structure plays a minor role. This tentative conclusion may be an oversimplification for such covalent materials as Si and Ge (cf. Fig. 7).

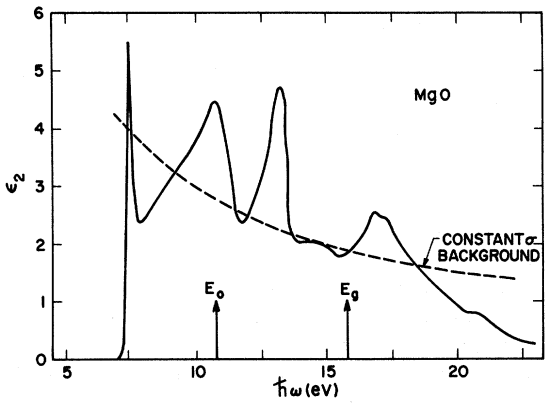

FIG. 6. Experimental ϵ_2 spectrum for MgO taken from Ref. 16 together with approximate constant-conductivity background and average energy gaps E_0 and E_g.

It is of interest to note that a constant-conductivity background with superimposed structure is predicted by theoretical arguments. The expression for the electronic conductivity is given by

$$\sigma(\omega) = (e^2\hbar/8\pi^2 m) \int_{BZ} d^3k\, f_{cv}(\vec{k})\delta[\mathcal{E}_c(\vec{k}) - \mathcal{E}_v(\vec{k}) - \hbar\omega], \quad (35)$$

where f_{cv} is the oscillator strength for transitions between valence and conduction bands, $\mathcal{E}_c$ and $\mathcal{E}_v$ are the conduction- and valence-band energies, and the integral extends over the Brillouin zone. In terms of an average oscillator strength $\bar{f}_{cv}$ and joint density-of-states function $\rho(\omega)$, Eq. (35) becomes

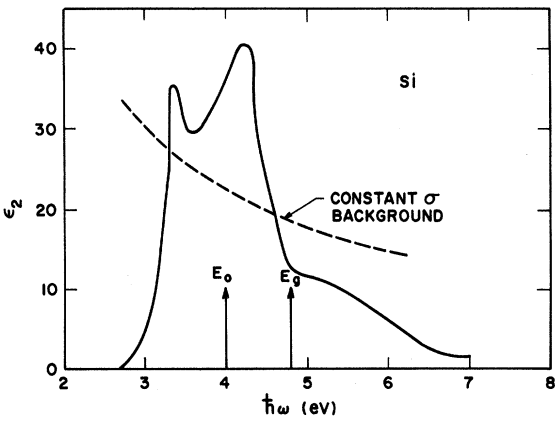

FIG. 7. Experimental ϵ_2 spectrum for Si taken from Ref. 17 together with approximate constant-conductivity background and average energy gaps E_0 and E_g.

$$\sigma(\omega) = (\pi e^2\hbar/2m)\, \bar{f}_{cv}\rho(\omega) \ . \tag{36}$$

By expanding $E_c(\vec{k}) - E_v(\vec{k})$ in Taylor series in the neighborhood of critical points, it can be shown that Eq. (36) reduces to

$$\sigma(\omega) \propto (\pi e^2\hbar/2m)\, \bar{f}_{cv}\, C + \sum_{\text{critical points}} + \sum_{\text{excitons}} , \tag{37}$$

where C is a constant related to transitions throughout the zone. The product $\bar{f}_{cv}C$ is, thus, a measure of the background conductivity.

The simplified model spectrum described by Eq. (30) contains an unknown bandwidth parameter b. In Ref. 3, we postulated that the normalized conductivity $(\sigma/N_cZ_aN_e)$ was the same in all ionic and covalent materials. As a consequence we derived a value $b_c \approx 3.4$ for covalent materials and $b_i \approx 2.1$ for ionic materials. Using Eqs. (20) and (34), we then found a "universal" value of σ given by

$$\sigma/N_cZ_aN_e = 80 \pm 12\ (\Omega\ \text{cm})^{-1} \ . \tag{38}$$

Our choice of a sharp upper-frequency cutoff described by the parameter b is, of course, unrealistic, although a rapid decrease in σ is expected at high frequencies because of exhaustion of the interband transitions and the form of the crystalline pseudopotential. Rather than distinguish between ionic and covalent crystals solely on the basis of bandwidth alone, we now postulate an alternative model spectrum in which the bandwidth is fixed and the conductivity, i.e., $\bar{f}_{cv}C$ in Eq. (37), is different in ionic and covalent crystal classes. Based on available experimental data in large numbers of crystals we take $b \approx 2.5$. Combining Eqs. (20)–(22) with (34) we obtain

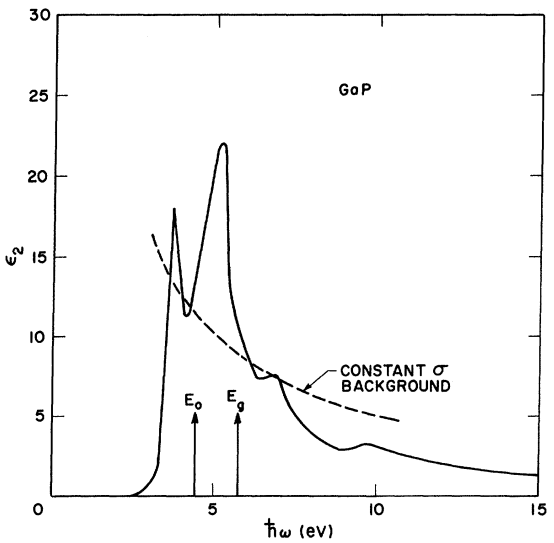

FIG. 8. Experimental ϵ_2 spectrum for GaP taken from Ref. 18 together with approximate constant-conductivity background and average energy gaps E_0 and E_g.

$$\sigma_i/N_cZ_aN_e = 70 \pm 10\ (\Omega\ \text{cm})^{-1}, \text{ ionic} \tag{39}$$

$$\sigma_c/N_cZ_aN_e = 100 \pm 15\ (\Omega\ \text{cm})^{-1}, \text{ covalent.} \tag{40}$$

Equation (30) then yields the relations

$$\epsilon_2 = (0.5 \pm 0.07)N_cZ_aN_e/E, \text{ ionic} \tag{41}$$

$$\epsilon_2 = (0.75 \pm 0.12)N_cZ_aN_e/E, \text{ covalent,} \tag{42}$$

where $E = \hbar\omega$ in units of electron volts, and $E_t < E < 2.5E_t$.

Equations (39)–(42) describe a simplified approximate dielectric model that correctly predicts both the magnitude and dispersion of refractive indices in more than 100 widely different substances. The only distinction between ionic and covalent materials using this constant-bandwidth model is the 50%-larger conductivity (or transition strength) observed in the covalent class. Crystal structure enters only through the nearest-neighbor coordination number N_c, chemistry through the anion valency Z_a, and valence-band structure through the equivalent number of electrons per anion N_e . To within the ±15% error limits, the model spectrum does not depend on the lattice constant or volume density. It should be pointed out that the choice of $N_e \equiv 8$ for filled s-p valence bands assumes that the s-p splitting is sufficiently small so that the bands derived from the atomic s-like anion orbitals can contribute to interband transitions over the range of energies of importance in determining E_0 and E_d . In the more ionic materials, energy-band computations[15,16] suggest that the s-like bands may lie so far below the p-like bands that this assumption is invalid, in which case it might be more appropriate to choose $N_e \approx 6$. In covalently bonded materials having sp^3 hybridized orbitals, all eight valence electrons contribute to the bonding. This observation could account for the approximately 50% lower transition strength observed in the ionic materials and would make Eqs. (40) and (42) apply to all materials – ionic as well as covalent.

We now turn to a comparison between the simplified dielectric model presented above and the ϵ_2 spectrum derived theoretically by Bardasis and Hone[13] based on the Penn model. The Penn-model ϵ_2 spectrum is given to a good approximation by[13]

$$\epsilon_2(\omega) = \frac{16}{3\alpha_0 k_F}\, \frac{E_F^2 E_g^2}{(\hbar\omega)^4}\, \frac{\hbar\omega}{[(\hbar\omega)^2 - E_g^2]^{1/2}}, \quad \hbar\omega > E_g \tag{43}$$

$$\epsilon_2 = 0, \quad \hbar\omega < E_g$$

where $\alpha_0 = 0.529$ Å is the Bohr radius, and k_F and E_F are the Fermi wave number and energy, respectively, of a free-electron gas having an electron density equal to that of the valence electrons. The spectrum is shown in Fig. 9 for Ge and compared with both the observed spectrum and the constant σ model. It is clear that the Penn spectrum bears

little resemblance to either the observed spectrum or the constant-σ model.

VIII. DISCUSSION

We have shown that a single oscillator having adjustable strength and position accurately describes the dispersion of the refractive index in more than 100 ionic and covalent materials (solids and liquids). The utility of such a simple result for large numbers of very different materials lies in the empirical rule obeyed by the dispersion energy parameter E_d. Through this quantity we find that ionicity, coordination number, and chemical valency play central roles in determining the behavior of refractive indices, and, as a consequence, electro-optic, nonlinear-optical, and photoelastic effects.[19,20] The dispersion energy properly normalizes the interaction potential describing these optical effects and, thus, directly influences their magnitudes.

Before discussing whether or not the empirical rules on E_d fall within the framework of existing theories, we now ask if there is some connection between the various parameters introduced by different authors to describe optical properties (viz., E_0, E_d, $\hbar\omega_p$, E_g, and E_a). We have shown that E_d obeys interesting empiricisms, while Phillips and Van Vechten[1] find widely applicable empiricisms associated with E_g. The other quantities of interest obey the f sum rule ($\hbar\omega_p$) and the Hopfield sum rule[4] (E_a). The latter sum rule, Eq. (16), is given by

$$E_a^2 = -\frac{e\hbar}{3mN_u}\int_{\text{all space}} \delta\rho(\vec{r})\,\nabla^2 V_b(\vec{r})\,d^3r, \tag{44}$$

where N_u is the number of electrons per unit cell, $\delta\rho(\vec{r})$ is the variation of the electron density in the crystal about the average, and $V_b(\vec{r})$ is the bare atomic-crystal potential. Physically, E_a is the natural frequency of the electronic charge clouds, treated as a rigid-charge density, vibrating against the atomic cores, whereas ω_p is the natural frequency of vibration of the free-valence-electron gas. We note that the sum-rule parameters $\hbar\omega_p$ and E_a describe the magnitude and dispersion of $\epsilon_1(\omega)$ at high frequencies above the cutoff of the ϵ_2 spectrum. Thus, according to Sec. III, the M_3 and M_1 moments determine the high-frequency behavior of ϵ_1. On the other hand, at low frequencies, below the bandgap, the magnitude and dispersion of $\epsilon_1(\omega)$ are determined by the M_{-1} and M_{-3} moments. Because different moments are involved, there is no general connection between the high- and low-frequency behavior of $\epsilon_1(\omega)$. A simple connection is obtained, however, if we choose the specific model ϵ_2 spectrum given by Eq. (30). For this constant-conductivity model the following expressions give the three energy gaps of interest:

$$E_a^2 = M_3/M_1 = \tfrac{1}{3}E_t^2(b^2+b+1), \tag{45}$$

$$E_g^2 = M_1/M_{-1} = E_t^2 b, \tag{46}$$

$$E_0^2 = M_{-1}/M_{-3} = E_t^2 3b^2/(b^2+b+1), \tag{47}$$

while the interband-strength parameters are given by

$$(\hbar\omega_p)^2 = 8\,(\hbar\sigma)E_t(b-1), \tag{48}$$

$$E_d^2 = 192(\hbar\sigma)^2(b-1)^2/(b^2+b+1). \tag{49}$$

Hopfield[4] has pointed out that these strength parameters are interrelated via the E_a gap [Eq. (45)] by

$$(\hbar\omega_p)^2 = E_a E_d\,. \tag{50}$$

It is also clear from Eqs. (45)–(47) that the three energy gaps are interrelated by

$$E_g^2 = E_a E_0\,. \tag{51}$$

We emphasize that Eqs. (50) and (51) are independent of *all* the parameters of the constant-conductivity model (σ, b, E_t). Within the framework of this model, then, the Hopfield gap E_a, as given by the sum rule Eq. (44), provides the connection between the Phillips parameters and the oscillator parameters E_0 and E_d. In Fig. 10 we show our model ϵ_2 spectrum for $b = 2.5$ and indicate the positions of the three energy gaps E_0, E_g, and E_a, as well as the plasma energy $\hbar\omega_p$. The $\epsilon_1(\omega)$ spectra at high and low frequencies are shown by the dashed lines, and the moments which determine these spectra are also indicated in parentheses. From the moment expressions for the quantities in Eqs. (50) or (51), it can be shown that

$$E_d^2 \equiv M_{-1}^3/M_{-3} = M_1^3/M_3\,. \tag{52}$$

Equation (52) holds for the constant-conductivity

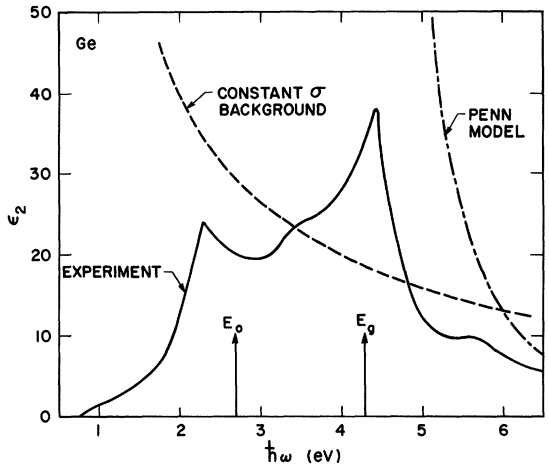

FIG. 9. Experimental ϵ_2 spectrum for Ge compared with results of Penn and constant-conductivity models. The energy gaps E_0 and E_g are also indicated.

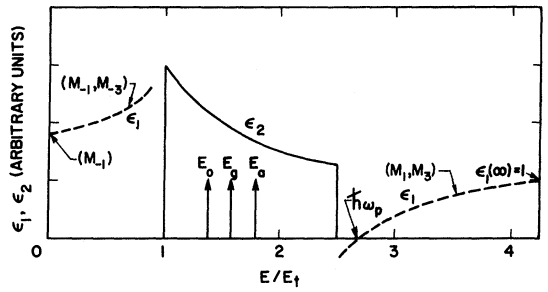

FIG. 10. Schematic illustration of the high- and low-frequency behavior of ϵ_1 (dashed lines) compared with the constant-conductivity model ϵ_2 spectrum (solid line). The moments determining ϵ_1 at high and low frequencies are indicated in parentheses.

model but is not generally valid for Aslaksen's[14] form of the ϵ_2 spectrum given by Eq. (31).

Either Eq. (50) or (51) can be used to determine experimental values of E_a using known values of E_g or $\hbar\omega_p$ and E_0 or E_d. Because of the empirical rule on E_d given by Eq. (20) and the proportionality between $(\hbar\omega_p)^2$ and the volume density of electrons, Eq. (50) provides a simple expression for E_a, i.e.,

$$E_a \approx 37\,(n_a \times 10^{-22})/N_c Z_a \text{ eV}, \tag{53}$$

where n_a is the volume density of *anions*, and we have taken $\beta = 0.37$ eV. It is not as yet clear, however, how Eq. (53) is contained within the Hopfield sum rule expressed by Eq. (44), although the form of Eq. (53) suggests that atomiclike nearest-neighbor quantities are of major importance.

Shaw[21] has recently introduced a "dispersion energy" analogous to E_d into the Phillips-Van Vechten description by defining the quantity

$$(E_d')^2 \equiv (\hbar\omega_p)^4/E_g^2 \equiv M_1 M_{-1}\,. \tag{54}$$

For the constant-conductivity model, Eqs. (46) and (48) then yield the relation

$$(E_d')^2 = 192\,(\hbar\sigma)^2\,(b-1)^2/3b. \tag{55}$$

Comparison with Eq. (49) shows that

$$(E_d/E_d')^2 = 3b/(b^2+b+1) \leq 1.$$

For a typical value of $b = 2.5$, $E_d' = 1.14E_d$. Shaw finds that both E_d and E_d' correlate in a simple way with the Phillips ionicity $f_i = C^2/E_g^2$, i.e., the dispersion energies are approximately proportional to $(1-f_i)$. According to Eqs. (49) and (55) this result implies, as pointed out by Shaw, that

$$\sigma^2 \propto (1-f_i), \tag{56}$$

that is, the conductivity decreases continuously with increasing ionicity. Thus far there do not appear to be clear-cut experimental or theoretical arguments that unambiguously support either the ionicity-related conductivity given by Eq. (56) or the two-valued form given by Eqs. (39) and (40).

In terms of the average oscillator strength $f(\omega)$ and joint density of states $\rho(\omega)$ Eqs. (20) and (36) yield the relation

$$\sigma \propto f\rho \propto \beta N_c Z_a N_e\,, \tag{57}$$

independent of the volume density of electrons to within ±15%. To our knowledge, none of the existing theories of optical properties explains the experimental observations described by Eq. (57). In no case do coordination number and valency enter in such a simple way, and in no case does the volume density of electrons fail to be an important quantity. In existing theories, as well as in the Phillips-Van Vechten model, the volume density enters naturally via the f sum rule (M_1 moment). Only the M_{-1} and M_{-3} moments determine E_d so that the higher-energy interband transitions that influence M_1 have little influence on E_d. However, within the confines of the constant-conductivity model Eq. (52) relates E_d to the sum-rule moments M_3 and M_1. As a result, the dispersion energy may depend upon the detailed charge distribution within each unit cell via Eq. (44) and, consequently, would then be closely related to chemical bonding. The dependence on N_c and Z_a suggests further that *nearest-neighbor* atomiclike quantities are of major importance, and that an understanding of the electronic optical properties of materials and their relationship to chemical bonding may lie within a nearly localized orbital theory.

ACKNOWLEDGMENTS

We wish to thank J. R. Brews and K. K. Thornber for helping to clarify several points in the manuscript, and acknowledge useful discussions with R. W. Shaw, Jr. We also wish to thank J. C. Phillips for reading the manuscript.

[1]J. C. Phillips, Phys. Rev. Letters 20, 550 (1968); J. C. Phillips and J. A. Van Vechten, *ibid.* 22, 705 (1969); J. A. Van Vechten, Phys. Rev. 182, 891 (1969).
[2]D. R. Penn, Phys. Rev. 128, 2093 (1962).
[3]S. H. Wemple and M. DiDomenico, Jr., Phys. Rev. Letters 23, 1156 (1969).
[4]J. J. Hopfield, Phys. Rev. B 2, 973 (1970).
[5]J. C. Philips, Rev. Mod. Phys. 42, 317 (1970).
[6]See, for example, J. R. Tessman, A. H. Kahn, and W. Shockley, Phys. Rev. 92, 890 (1953); and I. M. Boswarva, Phys. Rev. B 1, 1698 (1970).
[7]P. Noizières and D. Pines, Phys. Rev. 113, 1254 (1959).
[8]S. S. Batsanov, *Refractometry and Chemical Structure* (Consultants Bureau, New York, 1961).
[9]S. Kurtin, T. C. McGill, and C. A. Mead, Phys. Rev. Letters 22, 1433 (1969).
[10]D. E. Eastman, F. Holtzberg, and S. Methfessel,

Phys. Rev. Letters 23, 226 (1969).
[11]D. Eisenberg and W. Kauzmann, *Structure and Properties of Water* (Oxford U.P., Oxford, England, 1969).
[12]T. S. Moss, *Optical Properties of Semiconductors* (Butterworths, London, 1961).
[13]S. Bardasis and D. Hone, Phys. Rev. 153, 849 (1967).
[14]E. W. Aslaksen, Phys. Rev. Letters 24, 767 (1970).
[15]C. Y. Fong and M. L. Cohen, Phys. Rev. 185, 1168 (1968).
[16]C. Y. Fong, W. Saslow, and M. L. Cohen, Phys. Rev. 168, 992 (1968).
[17]D. Brust, Phys. Rev. 134, A1337 (1964).
[18]H. R. Philipp and H. Ehrenreich, Phys. Rev. 129, 1550 (1963).
[19]S. H. Wemple and M. DiDomenico, Jr., *Applied Solid State Science*, edited by R. Wolfe (Academic, New York, to be published), Vol. III.
[20]S. H. Wemple and M. DiDomenico, Jr., Phys. Rev. B 1, 193 (1970).
[21]R. W. Shaw, Jr., Phys. Rev. Letters 25, 818 (1970).

PHYSICAL REVIEW B VOLUME 3, NUMBER 4 15 FEBRUARY 1971

Far-Infrared Properties of Lattice Resonant Modes. V. Second-Order Stark Effect*

B. P. Clayman
Laboratory of Atomic and Solid State Physics, Cornell University, Ithaca, New York 14850
and
Department of Physics, Simon Fraser University, Burnaby 2, *British Columbia, Canada* †
and
R. D. Kirby‡ and A. J. Sievers§
Laboratory of Atomic and Solid State Physics, Cornell University, Ithaca, New York 14850
(Received 8 September 1970)

Small electric-field-induced frequency shifts have been observed for resonant modes associated with three defect systems. For NaI:Cl^-, the shifts have been used to measure the quartic anharmonic terms of the interionic potential of the impurity ion. For KBr:Li^+, the quartic anharmonic terms are found to be very small, and an harmonic potential which includes a central barrier with the barrier height less than the zero-point energy of the oscillator is required to explain the experimental results. For NaCl:Cu^+, only an "on-center" resonant-mode configuration is consistent with the experimental results.

I. INTRODUCTION

The response of lattice resonant modes in alkali-halide crystals to an external dc electric field is a sensitive probe of the local impurity environment. For a harmonic-oscillator resonant mode associated with an "on-center" defect, an applied electric field shifts all energy levels by the same amount, and no change in the far-infrared absorption frequency is to be expected. For paraelectric impurities, whose far-infrared properties are strongly modified by the tunneling motion of the "off-center" impurity ion, giant electric field effects have been observed.[1] We have measured small electric-field-induced frequency shifts associated with three "on-center" defect systems: NaI:NaCl, KBr:LiBr, and NaCl:CuCl. Because these experiments complement previous far-infrared measurements incorporating other perturbations,[2,3] some definite features of the anharmonic potentials which bind these impurities can now be resolved.

Of the three lattice-defect systems, the largest electric-field-induced frequency shifts have been observed in NaI:Cl^-. The resonant-mode frequency shifts have been used to determine the cubic symmetry of the defect site and to measure the quartic anharmonic terms of the interionic potential of the impurity ion. A preliminary description of these findings has been given earlier.[4]

The much smaller electric-field-induced shifts[5] observed for KBr:Li^+ are significant in that they eliminate the possibility that quartic anharmonic terms play an important role in the local potential of this defect. Both the small electric field shift and the large isotope shift previously observed[2] are explained with an harmonic potential containing a central barrier. The barrier is small compared to the zero-point energy of the resonant mode, hence the impurity still appears to occupy the normal equilibrium lattice site.

The null electric field effects observed for NaCl:Cu^+ are consistent with an "on-center" resonant-mode configuration. For this case, the exact shape of the potential has not been determined.